Research Article

Wei Wang#, Liping Liu#, Zhiying Han*

Effect of copper nanoparticles green-synthesized using *Ocimum basilicum* against *Pseudomonas aeruginosa* in mice lung infection model

https://doi.org/10.1515/chem-2024-0062
received April 19, 2024; accepted June 11, 2024

Abstract: The frequency of lung infection induced by multi-drug resistant strains of *Pseudomonas aeruginosa* has significantly risen, primarily due to the inadequate effectiveness of powerful chemotherapeutic methods. This study demonstrates that the *Ocimum basilicum* aqueous extract and copper nanoparticles (CuNPs) exhibited significant antioxidant and anti-infectious properties under *in vivo* conditions. To analyze the characteristics of the CuNPs synthesized from the reaction between copper nitrate solution and the aqueous *O. basilicum* extract, various techniques such as energy dispersive X-ray analysis, field emission scanning electron microscopy, Fourier transform infrared spectroscopy, X-ray diffraction analysis, and transmission electron microscopy were employed. The *in vivo* study encompasses the assessment of *P. aeruginosa* lethal dose in mice and the disease manifestation analysis, which comprises reduction in body weight, hypothermia, bacteremia, and other parameters, over a 48 h infection period. The infected mice exhibited a notable decrease in body temperature, measuring at 25°C after 48 h, compared to the initial temperature of 39°C. Additionally, a 30% reduction in weight was seen at the conclusion of the study. To assess the effectiveness of CuNPs on lung infection caused by the calculated lethal dose and bacteremia, histopathology analysis was employed. The bacterial load in the CuNPs group was determined to be 0.5 Log10CFU/mL on Day 8, indicating a notable decrease from the initial measurement of 1.5 Log10CFU/mL on Day 1. The histopathological findings revealed a widespread and sporadic buildup of alveolar space inflammatory cells, with infiltrates observed throughout all lung sections in infected mice. Enhanced lung histology was observed in the group of animal treated with reduced exudates noted at 200 μg/kg. CuNPs demonstrated inhibitory effects on the growth of *P. aeruginosa* at 8 μg/mL, while at 16 μg/mL, they effectively eradicated *P. aeruginosa*. The research unequivocally demonstrates the efficacy of CuNPs extract in combating lung infections induced by *P. aeruginosa* at 200 μg/kg. The recent survey aims to further explore the biomedical characteristics of these CuNPs in order to develop a powerful treatment against this dangerous pathogen.

Keywords: antioxidant, copper nanoparticles, lung infection, *Ocimum basilicum* leaf, *Pseudomonas aeruginosa*

1 Introduction

The respiratory system is regularly in contact with the outside environment, leading to potential exposure to various microorganisms like fungi, viruses, and bacteria in the air. If pathogenic microorganisms are not eliminated from the lungs upon inhalation, respiratory tract infections may develop. Lower respiratory tract infections are a significant concern, as they are the primary cause of death in developing nations and the third most common cause of death globally [1,2]. Furthermore, the global healthcare system is facing an increasing financial burden due to the need for intensive care caused by lower respiratory tract infections. Typically, bacteria are the primary culprits behind lower respiratory tract infections, but there is growing body of evidence offering that bacterial infections followed by viral infections are becoming more common [3–5]. Lower respiratory tract infections pose a significant challenge in terms of treatment due to the presence of microbes deeply entrenched within the respiratory tract. Typically, these microbes are nestled within a dense amalgamation of viscous mucus and biofilm, making eradication a formidable task. To effectively treat these infections, oral and/or intravenous antibiotics should be administered

# Wei Wang and Liping Liu contributed equally to this study.

*** Corresponding author: Zhiying Han**, Respiratory Department, Shanxi Children's Hospital, Taiyuan, 030013, China, e-mail: sxhanzhiying666@outlook.com, sxhanzhiying@hotmail.com
Wei Wang, **Liping Liu:** Respiratory Department, Shanxi Children's Hospital, Taiyuan, 030013, China

at high doses in order to be beneficial [4–6]. This is because only a small portion of drugs administered can reach the mucosal side of the lungs from systemic circulation. On the other hand, inhaling antimicrobials provides precise drug administration to the main infection site, while reducing overall exposure of the body and potential side effects [5,6]. It is imperative to maintain elevated levels of antimicrobials in the local area to successfully eliminate antibiotic-sensitive and multidrug-resistant pathogens, causing extracellular or intracellular infections. Nevertheless, solution-based inhaled antimicrobials frequently face the challenge of swift clearance from the lungs or deactivation by metabolic enzymes [7]. Consequently, their residence times are brief, leading to sub-optimal concentrations of antimicrobials. This, in turn, can contribute to the antimicrobial resistance emergence [8,9]. The limited intracellular bioavailability of numerous antimicrobials exacerbates this issue, frequently resulting in the ineffectiveness of treating intracellular infections [10].

The pharmaceutical sector might prioritize the development of efficient formulations for expired drug molecules over the invention of new antimicrobial compounds, as the scarcity of new antimicrobials presents considerable obstacles. Delivery technologies based on nanoparticles (NPs) are increasingly being seen as promising methods to overcome the constraints of traditional formulations given inhaled, injected, or orally [11,12]. Incorporating antimicrobial agents into NPs designed for inhalation safeguards against deactivation due to the severe conditions present in the lungs during chronic bacterial infections, such as pH fluctuations and enzyme activity. Reduced risk of adverse effects by minimizing the drug's exposure to the entire body; controlled and potentially extended drug release (e.g., prolonged retention in the lungs, resulting in enhanced patient compliance). Additionally, customized characteristics of the NPs could assist in surmounting a range of obstacles and resistance mechanisms by enhancing drug absorption into and reducing the bacterial cell efflux out; and simultaneous administration of various antimicrobial agents in a single NPs, potentially leading to bactericidal outcomes and hindering the antimicrobial resistance emergence in bacteria [11,12].

Copper, being a prevalent antimicrobial metal, eradicates the bacteria responsible for Legionnaires' disease, along with drug-resistant microorganisms. Viruses that impact the global health community, including the Middle East Respiratory Syndrome and the 2019 pandemic (SARS-CoV-2) have been proven to perish within minutes upon contact with pure copper [13–18]. Ahmadi et al. reported the *Juglans regia* green husk aqueous extracts biosynthesized CuNPs antiviral efficacy and the Cu and Fe NPs synergistic action on viruses [19]. Rai et al., as well as Patoo et al. [20,21], have also provided evidence supporting the metal oxide NPs synergistic impacts on SARS-CoV-2. Copper can induce harm to diverse cellular processes and exhibit cytotoxic effects, thereby serving as a potent inhibitor against microbes. Copper inflicts damage on microbial cells through producing reactive oxygen species (ROS) and the substitution or attachment to the original cofactors in metalloproteins [22]. Furthermore, copper plays a role in innate immunity by catalyzing the production of ROS during the bursting reaction in phagocytes, thereby boosting bactericidal activity in bacterial phagocytosis [23]. Copper-based NPs can inhibit microorganisms using a mechanism similar to that of other copper materials discussed earlier [24–26]. Numerous studies have demonstrated that NPs possess more potent antimicrobial properties compared to materials of regular size. However, the exact explanation for this phenomenon remains unclear at the current time. CuNPs possess a greater surface area and distinct crystal structure compared to other copper molecular materials. These NPs can impact the microbial cells' cellular components through unique mechanisms, resulting in enhanced antibacterial efficacy [27–32]. Copper-based NPs can dissolve at a quicker rate in solutions, resulting in the release of a higher concentration of metal ions. Consequently, this enhanced release of metal ions leads to a more potent antimicrobial effect [33]. Copper-containing NPs can simultaneously activate multiple antibacterial mechanisms. However, it is challenging for a single microorganism to develop multiple gene mutations in order to combat the diverse antimicrobial mechanisms of these NPs. As a result, the antimicrobial resistance likelihood remains low. Cu-containing NPs incorporated into various dental materials generally hinder the growth of microorganisms primarily by releasing the NPs and Cu ions. The antimicrobial mechanism of Cu-containing NPs involves generating ROS, disrupting cell membranes and walls, and interacting with DNA and proteins [34].

Throughout history, various scientists and physicians have employed a variety of herbs for the purpose of treating illnesses [35]. As a result of the increase in drug resistance and the chemosynthetic drug's adverse consequences, there has been a growing interest among researchers and the global population in plant metabolites/extracts and medicinal herbs [35–37]. This is attributed to its lack of toxicity and the numerous health advantages it offers when employed to treat illnesses in medical and clinical environments [35]. *Ocimum basilicum* is a plant that contains a variety of bioactive phytochemicals such as glycosides, steroids, cardiac glycosides, reducing sugars, saponins, tannins, flavonoids, phenolics, and alkaloids. It also exhibits a range of pharmacological activities, such as antiviral, wound healing, antioxidant, anti-inflammatory, antifungal, and antibacterial properties [35,38–41]. The plant extracts show great promise for utilization as medicinal

ingredients, showcasing a wide range of healing abilities such as antiviral, antifungal, antioxidant, wound healing, anti-inflammatory, and antibacterial properties [35]. The research conducted by Yibeltal et al., demonstrated that the flower oil extract exhibited the most potent antibacterial effects on *Staphylococcus aureus*, displaying the largest inhibition zone of 15.47 mm. Additionally, it showed the lowest minimum inhibitory concentration (MIC) at 0.09 µg/mL and a correspondingly minimal minimum bactericidal concentration (MBC) of 0.19 µg/mL [41].

According to the above explanations, in this research we investigated the effect of green-synthesized CuNPs using *O. basilicum* on *Pseudomonas aeruginosa* in mice lung infection model. Various methods including X-ray analysis (EDX), field emission scanning electron microscopy (FE-SEM), Fourier transform infrared spectroscopy (FT-IR), X-ray diffraction analysis (XRD), and transmission electron microscopy (TEM) were utilized to examine the properties of the CuNPs produced from the interaction of copper nitrate solution with the aqueous *O. basilicum* extract.

2 Experimental

2.1 Preparation of *O. basilicum* extract

The newly harvested leaves of *O. basilicum* were rinsed with running water to eliminate any impurities and dust, followed by drying in the shade to form the powder. To prepare the leaf extract, 20 g of powder was placed into a 0.3 L conical flask with 0.2 L of distilled water. The mixture was heated on a magnetic stirrer at 65°C for 60 min. Subsequently, it was filtered using Whatman filter paper (No. 1), and the resulting leaf filtrate was utilized for the silver NPs formulation [36,41].

2.2 Green formulation of CuNPs

To prepare 0.25 M $Cu(NO_3)_2{\cdot}3H_2O$ stock solution, *O. basilicum* (50 mL) was mixed with $Cu(NO_3)_2{\cdot}3H_2O$ stock solution (40 mL) and incubated at 25°C for 180 min. A significant remarkable change in color was observed in the reaction solution [19,25]. The CuNPs biosynthesis was confirmed by TEM, FE-SEM, FT-IR, and EDX.

2.3 Chemical characterization of CuNPs

FE-SEM was used for the examination of the structure and composition of CuNPs. The CuNPs size distribution was depicted in a histogram using imageJ software. The identification of various functional groups accountable for the stabilization and reduction of the formulated CuNPs was accomplished through FT-IR analysis, using the Cary 630 FTIR model from Tokyo, Japan. The FT-IR analysis was performed using the KBr technique, where a slice containing 0.3 g of formulated CuNPs mixed with KBr was formed under high pressure. TEM analysis was employed to investigate the structure of zinc NPs (ZnNPs) using a JEOL model JEM-1010 from Tokyo, Japan. The Shimadzu DX-700HS machine was used to perform EDX analysis to identify the elements [19,25].

2.4 *In vivo* experimental design

All animal experiments were carried out in compliance with the guidelines set forth by Payame Noor University of Kermanshah (No. 01/Z/G 1395/12/01) regarding the Ethical Care and Use of Laboratory Animals. These guidelines were approved by the Research Ethics Committee of the Ministry of Health and Medical Education on April 17, 2006, and are in accordance with the Helsinki Protocol (Helsinki, Finland, 1975).

During this experimental investigation, 60 male BALB/c mice weighing between 38 and 40 g were utilized. The mice were housed in a controlled setting with a temperature maintained between 20 and 24°C. It is important to highlight that all procedures carried out in this study adhered to ethical guidelines concerning using laboratory animals.

Sixty mice were selected for the research project and distributed randomly into three groups, with 20 mice in each group. These groups consisted of a control (Normal) group, an untreated group, and a group treated with CuNPs at 200 µg/kg. The mice were anesthetized using a local anesthesia of 2% xylocaine administered subcutaneously. Lung infection was induced via intratracheal route using a 29-gauge needle to deliver 100 mL of a bacterial cell suspension (10^5 CFU/mL) in the early-logarithmic phase. The CuNPs therapy began immediately after the onset of infection and administered twice daily with a time gap of 2 and 4 h after injection. The therapy involves an oral dosage of 200 µg/kg body weight and is sustained for 7 days. The bacteremia blood sample was assessed daily by collecting it and streaking it on an agar plate to determine the concentration of viable bacteria in CFU/mL. Additionally, both lungs were aseptically obtained and examined for histopathological analysis [42].

On the seventh day, mice were euthanized via cervical dislocation. The entire lungs were removed and preserved in

4% paraformaldehyde. Subsequently, the lungs underwent decalcification in 5% formic acid before being embedded in paraffin. Tissue samples (5 mm thick) were stained using hematoxylin–eosin and examined using an Olympus microscope from Tokyo, Japan (manufactured in Philippines). A grading system was employed to assess the severity and the state of the lungs in the examined groups. The assessment was made on a scale ranging from 0.5 to 4, where:

- 0.5 represented a minor condition
- 1 indicated mild severity
- 2 denoted moderate severity
- 3 signified severe severity
- 4 represented very severe severity [42]

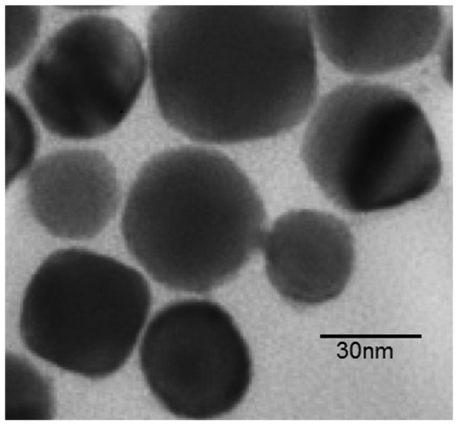

Figure 1: TEM image of CuNPs.

2.5 MIC and MBC tests

The MIC was determined using the macro-broth dilution technique. Tubes were filled with different concentrations of CuNPs, followed by the addition of 70 µL bacterial suspensions (*P. aeruginosa*) for incubation. Two essential factors for determining the MIC are the absence of turbidity and the lowest concentration. In order to establish the MBC, 70 µL of the MIC along with the four preceding wells were inoculated onto an Agar plate. The MBC is determined as the lowest concentration at which no bacterial growth is seen [25].

2.6 Statistical analysis

The normality of the data was assessed using Minitab-21. Following this, any data that were not normally distributed were transformed to achieve normality. The data variance analysis was carried out with SPSS-22, and graphical illustrations were generated using Excel software.

3 Results and discussion

3.1 Chemical characterization of CuNPs

One technique utilized to characterize metal NPs involves examining the electron microscope (FE-SEM) image, which are useful for analyzing the morphology of the produced NPs. The TEM and FE-SEM images captured from CuNPs under the specified ideal parameters reveal the production of spherical nanomaterials (Figures 1 and 2). The particles that were generated had a size of 10–50 nm. On an average, the NPs that were synthesized had a size between 20 and 30 nm. In terms of their morphology, the NPs exhibited crystalline geometric and uniform shapes. Additionally, due to the lengthy waiting time for analysis, the ZnNPs tended to agglomerate to some extent.

In agreement with our study, Kumar et al. [43] utilized leaves from the *Andean sacha* inchi plant to produce finely dispersed semi-crystalline CuNPs via a heating method. However, the size of CuNPs was found to be around 46 nm. On the other hand, Ananda Murthy et al. [44] successfully synthesized CuO NPs using an extract derived from *Vernonia amygdalina* Del. The monoclinic structure

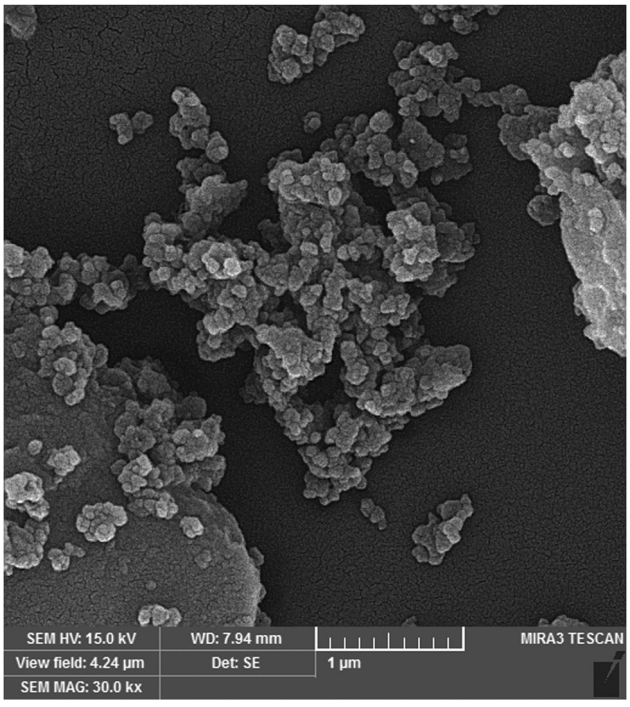

Figure 2: FE-SEM image of CuNPs.

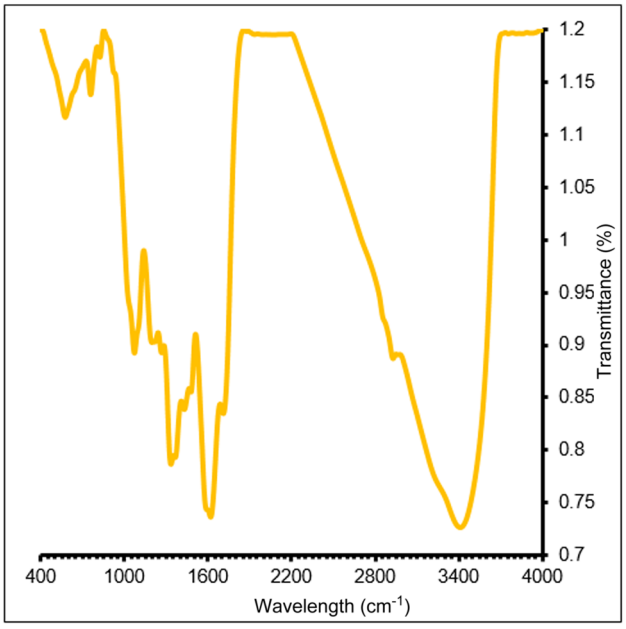

Figure 3: FT-IR analysis of CuNPs.

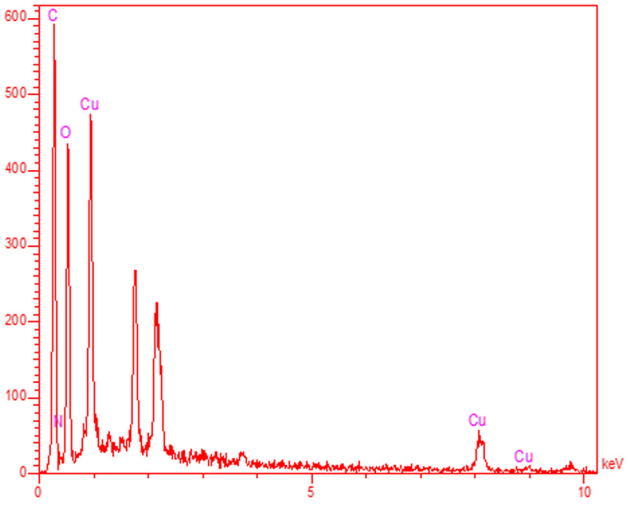

Figure 4: EDX analysis of CuNPs.

was observed in the synthesized NPs, which had a particle size measuring 19.7 nm. However, the synthesis of mixed Cu_2O/CuO NPs has not been extensively investigated until now. Gu et al. synthesized the CuNPs with *Calendula officinalis*, revealing a particle size below 100 nm [45]. Liyuan et al. found that the size of CuNPs formulated with *Alhagi maurorum* extract ranged from 10 to 60 nm [46]. Meanwhile, Chinnaiah et al. [47] synthesized CuNPs using *Datura metel* L. instead of CuO, and determined that the average crystallite size of the CuNPs was around 19.56 nm. In this investigation, CuNPs were prepared in a compact size. It is probably because the reduced size of CuNPs greatly enhances their therapeutic efficacies. Gu et al. [45] and Kumar et al. [43] have validated the remarkable therapeutic efficacies of CuNPs with small sizes, specifically ranging from 10 to 50 nm.

The metal–oxygen bond is associated with the bands below 700 cm^{-1} in FT-IR analysis. In Figure 3, the Cu–O bond is represented by a band at 582 cm^{-1}. The additional peaks at 1,067, 1,342–1,624, 2,929, and 3,412 correspond to the carbonyl (CO), C═C, CO_2, and hydroxyl (OH) organic functional groups of *O. basilicum*, respectively, which serve as the reducing agent during the synthesis process. Similar peaks related to the functional groups were reported in the studies of Kumar et al. [43], Ananda Murthy et al. [44], Gu et al. [45], and Chinnaiah et al. [47].

In the analysis conducted using EDX, the presence of copper in the biosynthesized CuNPs was confirmed by signals at 8.02 keV (for CuKα) and 0.93 keV (for CuLα), which were consistent with previous findings [16–19]. The formation of a signal around 0.5 keV can be associated with the oxygen present in CuNPs and certain organic molecules from the *O. basilicum* extract that are related to the CuNPs surface. Additionally, a signal at approximately 0.3 keV provides evidence of carbon on the CuNPs surface (Table 1; Figure 4). These findings are consistent with previous research performed by Gu et al. [45] and Liyuan et al. [46].

The evaluation of compounds' crystallinity can be done through the XRD diffraction pattern. Figure 5 displays the XRD pattern of CuNPs. The production of small-sized CuNPs with well-defined crystalline structure has been validated by these findings. The signal data obtained at various 2θ values were cross-referenced with the standard PDF card No. 04-012-7238 database. The (−111), (111), (−202),

Table 1: Quantitative results of the EDX elemental table

Elt	Line	Int	Error	K	Kr	W%	A%	ZAF	Formula	Ox%	Pk/Bg	Class	LConf	HConf	Cat#
C	Ka	356.2	9.5450	0.5100	0.2174	45.05	57.14	0.4825		0.00	158.77	A	43.54	46.55	0.00
N	Ka	10.9	9.5450	0.0201	0.0086	5.44	5.92	0.1575		0.00	17.14	A	4.40	6.48	0.00
O	Ka	268.8	9.5450	0.2211	0.0942	35.19	33.51	0.2678		0.00	90.56	A	33.84	36.54	0.00
Cu	Ka	63.2	0.7945	0.2488	0.1060	14.33	3.43	0.7403		0.00	8.32	A	13.19	15.46	0.00
				1.0000	0.4262	100.00	100.00			0.00					0.00

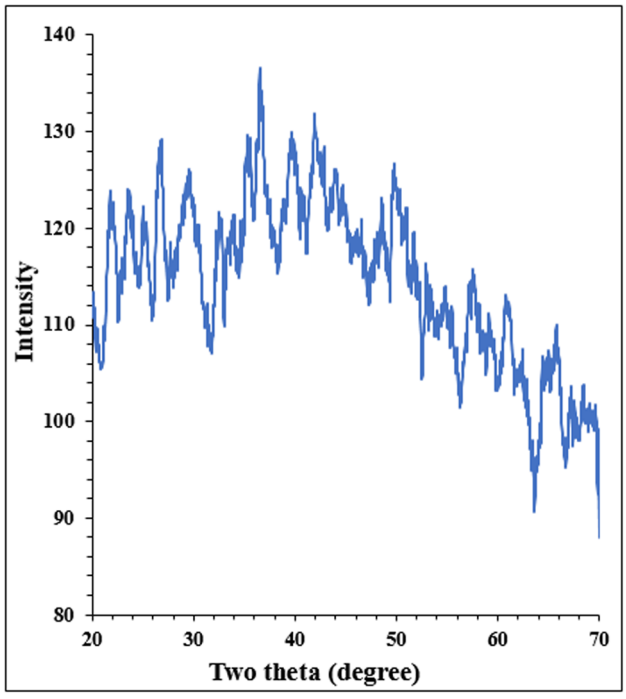

Figure 5: XRD analysis of CuNPs.

(202), (−113), (022), (−311), and (−221) planes are assigned to the signals at 35.77, 38.97, 48.88, 58.48, 61.68, 65.81, 66.41, and 68.24, respectively. These planes correspond to the data of copper oxide with the chemical formula CuO. The crystal size of CuNPs was determined through the application of Scherer's equation, yielding a measurement of 18.43 nm. Previous studies in the literature have reported a range of 12–40 nm for the crystal size of CuNPs [45–47].

The size distribution of CuNPs was analyzed using the dynamic light scattering technique. For this propose the CuNPs was dispersed in water. The analysis was performed using a dynamic light scattering instrument (Nanotrac wave II). The data are shown in Figure 1. According to the results, the average distribution size of NPs was less than 1,000 nm. Furthermore, an amount of −5.0 mV was calculated for the zeta potential. The particles with a zeta potential less than of ±30 mV usually show an aggregation property [11]. For CuNPs the result is in agreement with FE-SEM images (Figure 6).

3.2 Treatment of lung infection by CuNPs

The antimicrobial effects stem from the ion emission from copper, copper oxide, and nanoparticles, with the release speed being influenced by both the material's chemical composition and the presence of ROS and reactive nitrogen species. Various action mechanisms have been identified in the studies [48,49]. Cu ions impede the bacterial resistance emergence by employing multiple mechanisms at once. Bacterial membranes are damaged upon interacting with Cu surfaces. Cu ions have the capability to directly damage bacterial proteins and, through a Fenton-like reaction, produce highly ·OH that engage with various enzymes, DNA, and proteins, leading to the membrane structure disruption and lipid peroxidation [49–51]. CuO NPs have demonstrated the ability to facilitate favorable results, such as improved wound healing and angiogenesis. By modifying the surface through functionalization, the NP's surface charge can be changed, thereby aiding in the deactivation of bacteria. Positively charged NPs can bind more rapidly and effectively eliminate bacteria due to the negatively charged bacterial cell wall [48,50,51].

The *in vivo* investigation involves determining *P. aeruginosa* lethal dose in Swiss albino mice and evaluating disease symptoms such as weight loss, hypothermia,

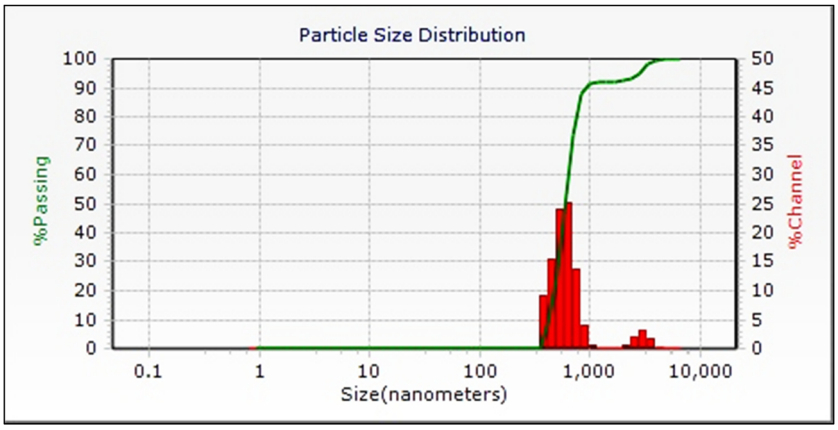

Figure 6: Size distribution histogram of CuNPs from dynamic light scattering analysis.

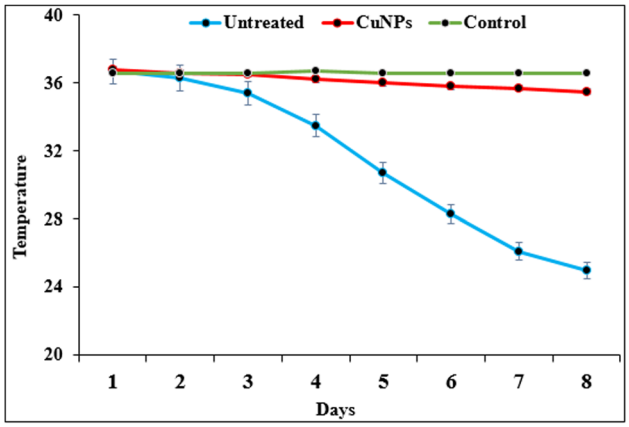

Figure 7: Efficacy of CuNPs on the body temperature of mice in several days.

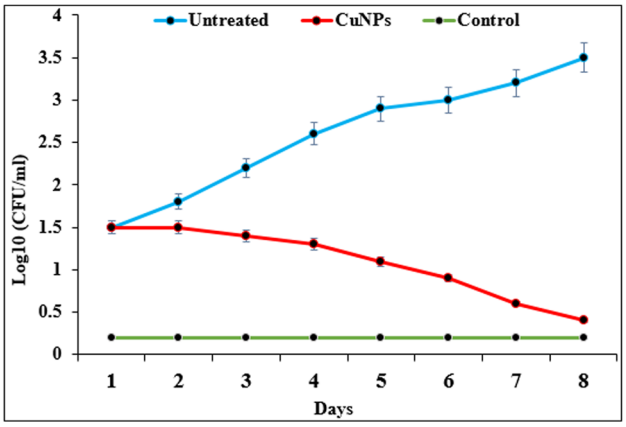

Figure 9: *In vivo* antibacterial efficacy of CuNPs in several days.

bacteremia, and other factors during a 48 h infection period. Following the infection, the mice indicated a notable drop in body temperature, reaching 25°C after 48 h, in contrast to the starting temperature of 39°C (Figure 7). Furthermore, a weight reduction of 30% was noted at the end of the research (Figure 8). In order to evaluate the efficiency of CuNPs in treating lung infection induced by the lethal dose and bacteremia, histopathology analysis was utilized. The bacterial count in the CuNPs group was found to be 0.5 Log10CFU/mL on the eighth day, showing a significant drop from the initial count of 1.5 Log10CFU/mL on the first day (Figure 9). The examination of tissue samples showed a widespread and irregular accumulation of alveolar space inflammatory cells, with infiltrates present in all lung sections of the infected mice. Improved lung tissue structure was evident in the treated group of animals, with decreased exudates observed at a dose of 200 µg/kg (Table 2). The study definitively proves the effectiveness of CuNPs extract in fighting lung infections caused by *P. aeruginosa* at 200 µg/kg.

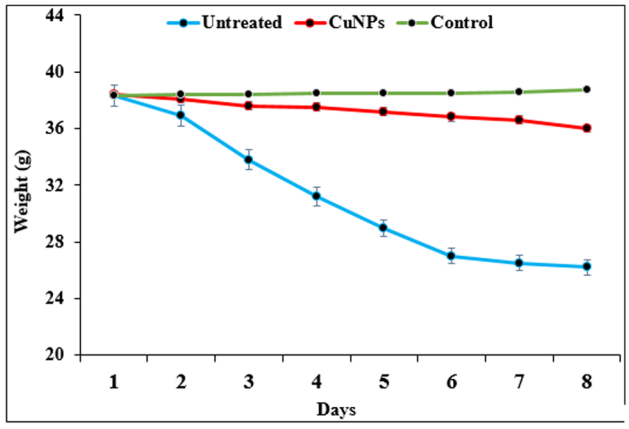

Figure 8: Efficacy of CuNPs on the body weight of mice in several days.

The recent research aims to further investigate the CuNPs biomedical properties to develop a potent treatment against this harmful pathogen.

Bacterial burden in mice blood collected at pre-decided time interval for the three groups for research.

At 8 µg/mL, CuNPs inhibited *P. aeruginosa* growth and effectively eliminated *P. aeruginosa* at 16 µg/mL (Table 3). The findings suggest that CuNPs possess notable antibacterial characteristics against *P. aeruginosa*.

Sandle [52] highlights that managing surfaces as carriers of pathogens is becoming an integral aspect of the comprehensive infection control approach. Numerous studies conducted in actual hospital environments have demonstrated that the presence of copper surfaces, when appropriately positioned, leads to a reduction of both bacterial contamination and infection rates [53]. Some research has shown that bacteria can be inactivated upon contact at

Table 2: Scoring of lung tissue histopathological examination

Criteria	Control	Untreated	CuNPs
Inflammatory cells infiltration in the alveolar space	0	3	1
Degeneration and distortion of alveoli	0	4	0
Inflammatory cell infiltration	0	3	1
Congestion	0	3	1
Total score	0	13	3

Table 3: MIC and MBC of CuNPs against *P. aeruginosa*

Microorganism	*P. aeruginosa*
MIC (µg/mL)	8 ± 0
MBC (µg/mL)	16 ± 0

7–8 log/h, resulting in the elimination of all microorganisms within a short time [54]. In 2010, a hospital in Birmingham, UK conducted a study that involved replacing certain surfaces with copper alloys. These alloys were utilized in an experimental composite toilet seat and other high-risk items like door locks, among others [55].

The data gathered demonstrate that the presence of bacteria on copper surfaces is significantly lower, ranging from 90 to 100%, compared to plastic and aluminum surfaces of similar nature. Numerous hospital facilities are now using copper alloys for touch surfaces like hospital cabinets, bed boards, tables, control buttons, switches, and door handles based on the available evidence [54–56]. Additionally, CuNPs are not only utilized on solid surfaces, but also certain companies are focusing on incorporating CuO NPs into textiles used for hospital pillowcases and beds, attire worn by patients and medical staff. A study conducted in intensive care units at Calama Hospital in Chile yielded comparable findings. An ambulatory investigation has verified the decrease in the presence of microorganisms, leading to a reduction of contamination near the Cu surfaces. The assessment indicates a 40% decline in infections acquired in the ICU, with the possibility of a reduction of up to 70%. After 6 h of exposure, the Cu-containing ZnO films resulted in a significant decrease in the quantity of viable *E. coli* in a medical facility setting [55–57]. This, in turn, contributes to lower care expenses and enhanced patient results [55,56].

Airborne pathogens pose a significant risk, as do surfaces. In hospitals, CuNPs are employed in air, ventilation, and heat conditioning systems. Generally, these systems utilize aluminum components. The outdoor air pollution design and levels can influence the growth of resilient biofilms made up of fungi and bacteria on various components such as air ducts, condensate drains, fins, and heat exchanger coils [58–60].

4 Conclusion

In a recent study, we checked the properties of CuNPs green formulation on lung infections. EDX, TEM, FT-IR, and FE-SEM tests were applied to determine the structural and morphological properties of NPs. The particles average diameter is 20–30 nm. The study outcomes indicated that copper NPs benefit in curing lung infections. The research has shown that CuNPs are highly effective in treating a *P. aeruginosa* multi-drug resistant strain in a mice lung infection model when administered orally at 200 µg/kg. Additionally, CuNPs resulted in a notable decrease in microbial load in the blood. It enables the dosage schedules formulation for its subsequent use in lung-protective capability, immunomodulatory capacity, and bactericidal effectiveness, which can be validated through complementary clinical trials conducted at the clinical stage.

Funding information: Authors state no funding involved.

Author contributions: Wei Wang: conceptualization, investigation, acquisition, formal analysis, data curation, methodology, validation, resources, writing – original draft, and writing – review & editing; Liping Liu: conceptualization, investigation, acquisition, project administration, methodology, validation, resources, writing – original draft, and writing – review & editing; Zhiying Han: conceptualization, investigation, acquisition, formal analysis, data curation, supervision, project administration, methodology, validation, resources, writing – original draft, and writing – review & editing.

Conflict of interest: Authors state no conflict of interest.

Ethical approval: The conducted research is not related to either human or animals use.

Data availability statement: The datasets generated during and/or analyzed during the current study are available from the corresponding author upon reasonable request.

References

[1] Wang H, Naghavi M, Allen C, Barber RM, Bhutta ZA, Carter A, et al. Global, regional, and national life expectancy, all-cause mortality, and cause-specific mortality for 249 causes of death, 1980–2015: a systematic analysis for the Global Burden of Disease Study 2015. Lancet. 2016;388(10053):1459–544.

[2] Troeger C, Blacker B, Khalil IA, Rao PC, Cao J, Zimsen SRM, et al. Estimates of the global, regional, and national morbidity, mortality, and aetiologies of lower respiratory infections in 195 countries, 1990–2016: a systematic analysis for the Global Burden of Disease Study 2016. Lancet Infect Dis. 2018;18(11):1191–210.

[3] van Doorn HR, Yu H. Viral respiratory infections. 05/28 ed. Hunter's tropical medicine and emerging infectious diseases. 2020. p. 284–8. doi: 10.1016/B978-0-323-55512-8.00033-8.

[4] Chakravarty M, Vora A. Nanotechnology-based antiviral therapeutics. Drug Deliv Transl Res. 2020;3:1–40.

[5] Andrade F, Rafael D, Videira M, Ferreira D, Sosnik A, Sarmento B. Nanotechnology and pulmonary delivery to overcome resistance in infectious diseases. Adv Drug Deliv Rev. 2013;65(13–14):1816–27.

[6] Klinger-Strobel M, Lautenschlager C, Fischer D, Mainz JG, Bruns T, Tuchscherr L, et al. Aspects of pulmonary drug delivery strategies for infections in cystic fibrosis–where do we stand? Expert Opin Drug Deliv. 2015;12(8):1351–74.

[7] Dudley MN, Loutit J, Griffith DC. Aerosol antibiotics: considerations in pharmacological and clinical evaluation. Curr Opin Biotechnol. 2008;19(6):637–43.
[8] Hoffman LR, D'Argenio DA, MacCoss MJ, Zhang Z, Jones RA, Miller SI. Aminoglycoside antibiotics induce bacterial biofilm formation. Nature. 2005;436(7054):1171–5.
[9] Drenkard E, Ausubel FM. Pseudomonas biofilm formation and antibiotic resistance are linked to phenotypic variation. Nature. 2002;416:740–3.
[10] Abed N, Couvreur P. Nanocarriers for antibiotics: a promising solution to treat intracellular bacterial infections. Int J Antimicrob Agents. 2014;43(6):485–96.
[11] Mahdavi B, Paydarfard S, Rezaei-Seresht E, Baghayeri M, Nodehi M. Green synthesis of NiONPs using *Trigonella subenervis* extract and its applications as a highly efficient electrochemical sensor, catalyst, and antibacterial agent. Appl Organomet Chem. 2021 Aug;35(8):e6264.
[12] Huh AJ, Kwon YJ. Nanoantibiotics": a new paradigm for treating infectious diseases using nanomaterials in the antibiotics resistant era. J Control Rel. 2011;156(2):128–45.
[13] Vincent M, Duval RE, Hartemann P, Engels-Deutsch M. Contact killing and antimicrobial properties of copper. J Appl Microbiol. 2018;124:1032–46.
[14] Hutasoit N, Kennedy B, Hamilton S, Luttick A, Rashid RAR, Palanisamy S. Sars-CoV-2 (COVID-19) inactivation capability of copper-coated touch surface fabricated by cold-spray technology. Manuf Lett. 2020;25:93–7.
[15] Merkl P, Long S, McInerney GM, Sotiriou GA. Antiviral activity of silver, copper oxide and zinc oxide nanoparticle coatings against SARS-CoV-2. Nanomaterials. 2021;11:1312.
[16] Jagaran K, Singh M. Nanomedicine for COVID-19: potential of copper nanoparticles. Biointerface Res Appl Chem. 2021;11:10716–28.
[17] Poggio C, Colombo M, Arciola CR, Greggi T, Scribante A, Dagna A. Copper-alloy surfaces and cleaning regimens against the spread of SARS-CoV-2 in dentistry and orthopedics. From fomites to anti-infective nanocoatings. Materials. 2020;13:3244.
[18] Ramos-Zúñiga J, Bruna N, Pérez-Donoso JM. Toxicity mechanisms of copper nanoparticles and copper surfaces on bacterial cells and viruses. Int J Mol Sci. 2023;24:10503.
[19] Ahmadi M, Elikaei A, Ghadam P. Antiviral activity of biosynthesized copper nanoparticle by *Juglans regia* green husk aqueous extract and iron nanoparticle: molecular docking and in-vitro studies. Iran J Microbiol. 2023;15:138–48.
[20] Rai M, Deshmukh SD, Ingle AP, Gupta IR, Galdiero M, Galdiero S. Metal nanoparticles: the protective nanoshield against virus infection. Crit Rev Microbiol. 2016;42:46–56.
[21] Patoo TS, Khanday F, Qurashi A. Prospectus of advanced nanomaterials for antiviral properties. Mater Adv. 2022;3:2960–70.
[22] Fu Y, Chang F, Giedroc DP. Copper transport and trafficking at the host–bacterial pathogen interface. Acc Chem Res. 2014;47(12):3605–13.
[23] Djoko KY, Ong CLY, Walker MJ, Mcewan AG. The role of copper and zinc toxicity in innate immune defense against bacterial pathogens. J Biol Chem. 2015;290(31):18954–61.
[24] Denluck L, Wu F, Crandon LE, Harper B, Harper S. Reactive oxygen species generation is likely a driver of copper-based nanomaterial toxicity. Environ Sci. 2018;5(6):1473–81.
[25] Pramanik A, Laha D, Bhattacharya D, Pramanik P, Karmakar P. A novel study of antibacterial activity of copper iodide nanoparticle mediated by DNA and membrane damage. Colloids Surf B Biointerfaces. 2012;96:50–5.
[26] Ulloa-Ogaz AL, Piñón-Castillo HA, Muñoz-Castellanos LN, Athie-García MS, Orrantia-Borunda E. Oxidative damage to *pseudomonas aeruginosa* atcc 27833 and *Staphylococcus aureus* atcc 24213 induced by CuO-NPs. Environ Sci Pollut Res Int. 2018;24(27):22048–60.
[27] Yuzer B, Aydın MI, Con AH, Inan H, Can S, Selcuk H, et al. Photocatalytic, self-cleaning and antibacterial properties of Cu(II) doped TiO. J Environ Manage. 2021;302:114023–33.
[28] Bao S, Lu Q, Fang T, Dai H, Zhang C. Assessment of the toxicity of cuo nanoparticles by using *Saccharomyces cerevisiae* mutants with multiple genes deleted. Appl Environ Microbiol. 2015;81(23):8098–107.
[29] Mutalik C, Okoro G, Krisnawati DI, Jazidie A, Rahmawati EQ, Rahayu D, et al. Copper sulfide with morphology-dependent photodynamic and photothermal antibacterial activities. J Colloid Interface Sci. 2021;607:1825–35.
[30] Morsy EA, Hussien AM, Ibrahim MA, Farroh KY, Hassanen EI. Cytotoxicity and genotoxicity of copper oxide nanoparticles in chickens. Biol Trace Elem Res. 2021;23(1):1–15.
[31] Wang X, Wang WX. Cu-based nanoparticle toxicity to zebrafish cells regulated by cellular discharges. Environ Pollut. 2021;292:118296–316.
[32] Tsymbal SA, Moiseeva AA, Agadzhanian NA, Efimova SS, Markova AA, Guk DA, et al. Copper-containing nanoparticles and organic complexes: metal reduction triggers rapid cell death via oxidative burst. Int J Mol Sci. 2021;22(20):11065–84.
[33] Karlsson HL, Cronholm P, Hedberg Y, Tornberg M, De Battice L, Svedhem S, et al. Cell membrane damage and protein interaction induced by copper containing nanoparticles—importance of the metal release process. Toxicology. 2013;313(1):59–69.
[34] Wang L, Hu C, Shao L. The antimicrobial activity of nanoparticles: present situation and prospects for the future. Int J Nanomed. 2017;12:1227–49.
[35] Zhakipbekov K, Turgumbayeva A, Akhelova S, Bekmuratova K, Blinova O, Utegenova G, et al. Antimicrobial and other pharmacological properties of *Ocimum basilicum*, Lamiaceae. Molecules. 2024;29(2):388.
[36] Ababutain IM. Antimicrobial activity and gas chromatography-mass spectrometry (GC-MS) analysis of Saudi Arabian *Ocimum basilicum* leaves extracts. J Pure Appl Microbiol. 2019;13:61.
[37] Backiam ADS, Duraisamy S, Karuppaiya P, Balakrishnan S, Sathyan A, Kumarasamy A, et al. Analysis of the main bioactive compounds from *Ocimum basilicum* for their antimicrobial and antioxidant activity. Biotechnol Appl Biochem. 2023;70:2038–51.
[38] Stanojevic LP, Marjanovic-Balaban ZR, Kalaba VD, Stanojevic JS, Cvetkovic DJ, Cakic MD. Chemical composition, antioxidant and antimicrobial activity of basil (*Ocimum basilicum* L.) essential oil. J Essent Oil Bear Plants. 2017;20:1557–69.
[39] Sahu A, Nayak G, Bhuyan SK, Bhuyan R, Kar D, Kuanar A. Antioxidant and antimicrobial activities of *Ocimum basilicum* var. thyrsiflora against some oral microbes. Multidiscip Sci J. 2024;6:2024026.
[40] Tarayrah H, Akkawi M, Yaghmour R. Investigations of the Palestinian medicinal plant basil (*Ocimum basilicum*): antioxidant, antimicrobial activities, and their phase behavior. Pharm Pharmacol Int J. 2022;10:97–104.
[41] Yibeltal G, Yusuf Z, Desta M. Physicochemical properties, antioxidant and antimicrobial activities of Ethiopian sweet basil (*Ocimum basilicum* L.) leaf and flower oil extracts. Recent Adv Anti-Infect

Drug Discov Former Recent Pat Anti-Infect Drug Discov. 2022;17:131–8.
[42] Chakotiya AS, Tanwar A, Srivastava P, Narula A, Sharma RK. Effect of aquo-alchoholic extract of *Glycyrrhiza glabra* against *Pseudomonas aeruginosa* in mice lung infection model. Biomed Pharmacother. 2017 Jun;90:171–8.
[43] Kumar B, Smita K, Debut A, Cumbal L. Andean sacha Inchi (*Plukenetia volubilis* L.) leaf-mediated synthesis of Cu_2O nanoparticles: a low-cost approach. Bioengineering (Basel, Switz). 2020;7:1–10.
[44] Ananda Murthy HC, Zeleke TD, Tan KB, Ghotekar S, Alam MW, Balachandran R, et al. Enhanced multifunctionality of CuO nanoparticles synthesized using aqueous leaf extract of *Vernonia amygdalina* plant. Results Chem. 2021;3:100141.
[45] Gu J, Aidy A, Goorani S. Anti-human lung adenocarcinoma, cytotoxicity, and antioxidant potentials of copper nanoparticles green-synthesized by *Calendula officinalis*. J Exp Nanosci. 2022;17(1):285–96.
[46] Liyuan T, Lijun Z, Wei H, Meixuan J, Man Z, Zhihui Y, et al. Green synthesised CuNPs using *Alhagi maurorum* extract and its ability to amelioration of *Mycoplasma pneumoniae* infected pneumonia mice model. J Exp Nanosci. 2022;17(1):585–98.
[47] Chinnaiah K, Maik V, Kannan K, Potemkin V, Grishina M, Gohulkumar M, et al. Experimental and theoretical studies of green synthesized Cu_2O nanoparticles using *Datura metel* L. J Fluoresc. 2022;1:1–10.
[48] Ivanova I, Stoyanova D, Nenova E, Staneva A, Kostadinova A. Antimicrobial and cytotoxic properties of metal and graphene nanomaterials (review). J Chem Technol Metall. 2020;55:239–50.
[49] Villapún V, Dover L, Cross A, González S. Antibacterial metallic touch surfaces. Materials. 2016;9:736.
[50] Leyland NS, Podporska-Carroll J, Browne J, Hinder SJ, Quilty B, Pillai SC. Highly efficient F, Cu doped TiO_2 anti-bacterial visible light active photocatalytic coatings to combat hospital-acquired infections. Sci Rep. 2016;6:24770.
[51] Rtimi S, Giannakis S, Sanjines R, Pulgarin C, Bensimon M, Kiwi J. Insight on the photocatalytic bacterial inactivation by co-sputtered TiO_2-Cu in aerobic and anaerobic conditions. Appl Catal B Environ. 2016;182:277–85.
[52] Sandle T. Risk management library volume 4: Practical approaches to risk assessment and management problem solving: tips and case studies. River Grove, IL, USA: DHI Publishing, LLC; 2018.
[53] Salgado CD, Sepkowitz KA, John JF, Cantey JR, Attaway HH, Freeman KD, et al. Copper surfaces reduce the rate of healthcare-acquired infections in the intensive care unit. Infect Control Hosp Epidemiol. 2013;34:479–86.
[54] Santo CE, Lam EW, Elowsky CG, Quaranta D, Domaille DW, Chang CJ, et al. Bacterial killing by dry metallic copper surfaces. Appl Environ Microbiol. 2011;77:794–802.
[55] Efstathiou G, Papastavrou E, Raftopoulos V, Merkouris A. Factors influencing nurses' compliance with standard precautions in order to avoid occupational exposure to microorganisms: a focus group study. BMC Nurs. 2011;10:1.
[56] Khan HA, Baig FK, Mehboob R. Nosocomial infections: epidemiology, prevention, control and surveillance. Asian Pac J Trop Biomed. 2017;7:478–82.
[57] Abraham J, Dowling K, Florentine S. Can copper products and surfaces reduce the spread of infectious microorganisms and hospital-acquired infections? Materials. 2021;14:3444.
[58] Montero DA, Arellano C, Pardo M, Vera R, Gálvez R, Cifuentes M, et al. Antimicrobial properties of a novel copper-based composite coating with potential for use in healthcare facilities. Antimicrob Resist Infect Control. 2019;8:3.
[59] Schmidt M, Bréchot N, Hariri S, Guiguet M, Luyt CE, Makri R, et al. Nosocomial infections in adult cardiogenic shock patients supported by venoarterial extracorporeal membrane oxygenation. Clin Infect Dis. 2012;55:1633–41.
[60] Pontin KP, Borges KA, Furian TQ, Carvalho D, Wilsmann DE, Cardoso HRP, et al. Antimicrobial activity of copper surfaces against biofilm formation by *Salmonella enteritidis* and its potential application in the poultry industry. Food Microbiol. 2021;94:103645.